

Reaction of Cr Atoms with O₂ at Low Pressures: Observation of New Chemiluminescence Bands from CrO₂*

Hyung Su Son and Ja Kang Ku*

*Department of Chemistry, Center for Integrated Molecular Systems,
Pohang University of Science and Technology, Pohang 790-784, Korea
Received November 14, 2003*

Ground and low-lying electronic states of Cr atoms in the gas phase were generated from photolysis of Cr(CO)₆ vapor in He or Ar using an unfocussed weak UV laser pulse and their reactions with O₂ and N₂O were studied. When 0.5-1.0 Torr of Cr(CO)₆/O₂/He or Ar mixtures were photolyzed using 295-300 nm laser pulses, broadband chemiluminescence peaked at ~420 and ~500 nm, respectively, was observed in addition to the atomic emissions from z⁷P^o, z⁵P^o, and y⁷P^o states of Cr atoms. When N₂O was used instead of O₂, no chemiluminescence was observed. The chemiluminescence intensities as well as the LIF intensities for those three low-lying electronic states (a⁷S₃, a⁵S₂ and a⁵D₁) showed second-order dependence on the photolysis laser power. Also, the chemiluminescence intensities were first-order in O₂ pressure, but the presence of excess Ar showed a strong inhibition effect on them. Based on the experimental results, the chemiluminescent species in this work is attributed to CrO₂* generated from hot ground state Cr atoms with O₂. The apparent radiative lifetimes of the chemiluminescent species and collisional quenching rate constants by O₂ and Ar also were investigated.

Key Words : Cr atoms, Chemiluminescence, CrO₂*

Introduction

Reactions of transition metal (TM) atoms in the gas phase with O₂ and oxygen containing molecules have drawn substantial interest during the past two decades, and have been an area of continuing research.¹⁻³ Many research groups have studied the influence of the ground and low-lying electronic states on the reactivity of TM atoms in oxidation reactions.⁴⁻¹² It has been reported that Sc, Ti and V atoms evaporated from a hot crucible react with O₂ or other oxygen containing molecules to produce chemiluminescent TM oxides, and the vibrational structures of the chemiluminescence (CL) spectra have been analyzed.¹³⁻¹⁵ Ritter and Weisshaar have studied reactions of the ground state Sc, Ti, and V atoms with OX (X=N, O, N₂) at 300 K. They found that all the exothermic O atom transfer reactions were very inefficient.¹⁶

Parnis and co-workers generated the ground state Cr atoms by multiphoton dissociation of Cr(CO)₆ at 559 nm and studied reactions of ground state Cr atoms with O₂ and other oxygen containing molecules under pseudo-first-order conditions at 298 K.¹⁷ They observed relatively fast removal rate of the ground state Cr atoms which depended on the O₂ pressure as well as on the total pressure. However, they did not observe CL as well as laser-induced fluorescence from CrO(X⁵P).

In the previous report, we have shown that the ground state FeO molecules can be generated easily at room temperature by photolyzing Fe(CO)₅ vapor in a Fe(CO)₅/O₂ or N₂O/He mixture using unfocussed weak UV laser pulses, and suggested that the highly unsaturated Fe(CO)_x fragments can react with O₂ or N₂O to generate ground state FeO molecules.¹⁸

We have applied the same method to look for the formation of the ground state CrO by photolyzing Cr(CO)₆/O₂ (or N₂O)/He (or Ar) mixtures. Indeed, we have identified the formation of the ground state CrO from the reaction of highly unsaturated Cr(CO)_x fragments with O₂ and N₂O by observing laser-induced fluorescence (LIF) signal from CrO(B⁵Π_Ω) ← CrO(X⁵Π_Ω) transition and reported depletion kinetics of the ground state CrO.¹⁹ During the kinetic study of the ground state CrO, we discovered a very broad structureless CL spectrum when the low pressure Cr(CO)₆/O₂/He or Ar mixtures were photolyzed.

In the present work, we report studies on the CL signal observed from photolyzing Cr(CO)₆ vapors in the Cr(CO)₆/O₂/He or Ar gas mixtures. The dependence of CL intensities on the photolysis laser power, O₂ and Ar pressures, and optical pumping results strongly support that the emitting species is CrO₂* generated from the hot ground state Cr atoms with O₂.

Experimental Method

An experimental setup used for this work is basically the same as that reported previously.¹⁸ The reaction cell was made of a 1 L Pyrex bulb and two-pairs of 2.5 cm Pyrex O-ring joints were attached to the bulb for the laser beam path and for the connection to a gas handling vacuum rack. A premixture of 10% O₂ in He or in Ar was slowly flowed through over Cr(CO)₆ powder at 273 K to entrap the Cr(CO)₆ vapor, and the resulting gas mixture was introduced to the photolysis/LIF cell. A typical flow rate of the gas mixture in the reaction cell was 0.2 mmol min⁻¹. The actual Cr(CO)₆ vapor pressure in the flowing cell was estimated to

be about 2.5 mTorr under our experimental conditions by comparing the LIF intensities of the ground state Cr atoms with those from premixtures of known compositions. The total pressure in the cell was controlled by adjusting the openings of an inlet needle valve and an exit Teflon valve. When the pressure in the cell was stabilized, unfocused UV laser pulses in the 290-300 nm regions were directed to the cell. The pulse energy of the photolysis laser (Quantel YG681-TDL50 with NBP, 8 ns) was 0.7-1.0 mJ/pulse and the beam diameter was 7 mm. However, the pulse energies of the photolysis laser were varied from 0.30 mJ to 1.60 mJ to investigate the power dependence of CL and the atomic emission signals.

A photolysis and probe method was employed for LIF experiments. The pulse energy and line width of the probe laser (Quantel YG581-TDL60 with NBP and DGO) were 0.1-0.2 mJ/pulse and $\sim 0.1 \text{ cm}^{-1}$, respectively, at the frequency doubled wavelength.

The CL signal and the LIF intensities were monitored at the right angle with respect to the laser beam direction by using a 50 cm monochromator (Spex 1870C) equipped with a holographic grating and a Hamamatsu R928 photomultiplier (PM) tube. The signal from the PM tube was digitized with a transient digitizer (Tektronix 7912HB) and transferred to a laboratory computer for signal averaging and storage.

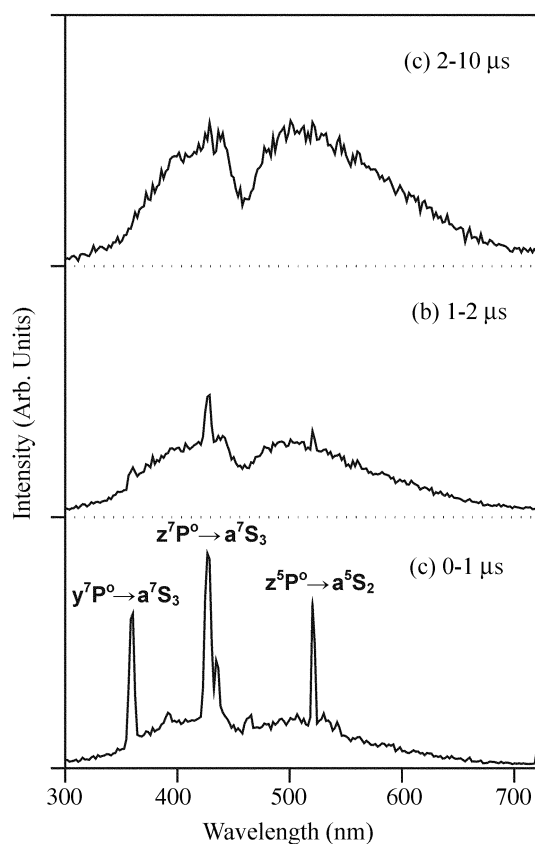


Figure 1. Time-resolved CL spectra observed from photolysis of a $\text{Cr}(\text{CO})_6/\text{O}_2/\text{He}$ mixture using unfocused UV laser pulses; (a) 0-1 μs , (b) 1-2 μs , and (c) 2-10 μs . The $\text{Cr}(\text{CO})_6$ vapor was entrapped by flowing a premixture of 10% O_2 in He and total pressure was 0.5 Torr.

Results

A. Chemiluminescence spectrum. When 0.5-1.0 Torr of $\text{Cr}(\text{CO})_6/\text{O}_2/\text{He}$ or Ar mixtures were photolyzed using unfocused weak UV laser pulses in the 290-300 nm region, broad band CL was observed in the 350-700 nm region as plotted in Figure 1. The sharp features at 360, 425 and 520 nm correspond to Cr atomic emission from y^7P^0 , z^7P^0 and z^5P^0 state, respectively.^{20,21} These three atomic emissions were always observed in addition to the dominant generation of the ground state Cr atoms under our experimental conditions supporting two distinctive photodissociation mechanism for $\text{Cr}(\text{CO})_6$ reported by Tyndall and Jackson.²² The atomic emissions disappeared within 2 μs , while the CL was observed for longer than 10 μs . Note that the apparent long duration of the atomic emissions is due to the long sampling time of the transient digitizer to catch relatively weak CL signal appearing in late time, and real atomic emissions disappeared within 150 ns at shorter time resolution of the transient digitizer. When N_2O was used instead of O_2 , or a $\text{Cr}(\text{CO})_6/\text{He}$ mixture was photolyzed without O_2 , only the three atomic emissions were detected, and no CL signal was observed. The three atomic emission intensities showed third-order dependence upon the photolysis laser power.

The CL spectra in Figure 1 show structureless continuum emissions peaked at around 400 and 500 nm, respectively. Efforts to resolve any vibrational band structures by increasing spectral resolution of the monochromator were unsuccessful. Thus, the nature of the emitting species seems

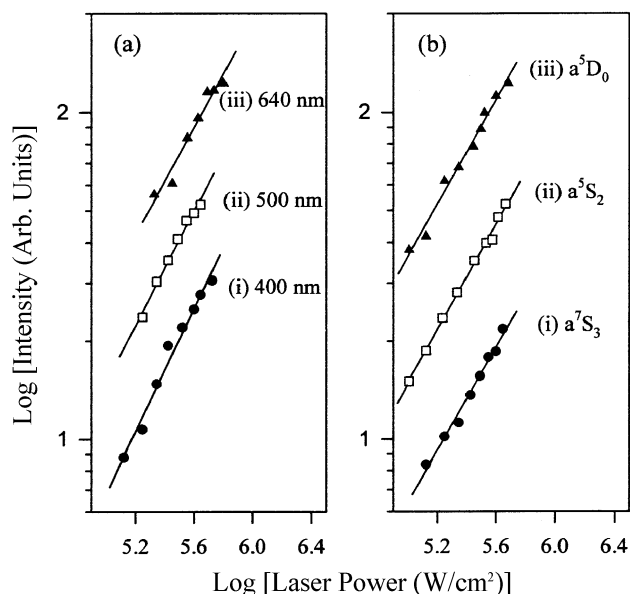


Figure 2. (a) Dependence of CL signal intensities on the photolysis laser power monitored at three different wavelengths. The magnitude of the slopes is (i) 2.1 ± 0.2 , (ii) 2.0 ± 0.2 , and (iii) 1.9 ± 0.2 , respectively. (b) Dependence of LIF intensities for the low-lying atomic states of Cr atoms on the photolysis laser power. The magnitude of the slopes is (i) 1.8 ± 0.2 , (ii) 1.9 ± 0.2 , and (iii) 1.9 ± 0.2 , respectively. To avoid congestion, plot (ii) and (iii) are vertically shifted.

Table 1. Excitation and monitored wavelengths for photolysis laser power dependence

	$\lambda_{\text{photolysis}}$ (nm)	λ_{exc} (nm) (Transition)	λ_{obs} (nm) (Transition)	Power dependence
CL	295.3 ^a	—	400	2.1 ± 0.2
Signal			500	2.0 ± 0.2
			640	1.9 ± 0.2
Cr(<i>a</i> ⁷ S ₃)	295.3	373.2 (<i>z</i> ⁵ P ₃ ^o ← <i>a</i> ⁷ S ₃)	520.8 (<i>z</i> ⁵ P ₃ ^o → <i>a</i> ⁵ S ₂)	1.8 ± 0.2
Cr(<i>a</i> ⁵ S ₂)	295.3	387.0 (<i>z</i> ⁵ D ₁ ^o ← <i>a</i> ⁵ S ₂)	392.1 (<i>z</i> ⁵ D ₁ ^o → <i>a</i> ⁵ D ₂)	1.9 ± 0.2
Cr(<i>a</i> ⁵ D ₁)	295.3	389.4 (<i>z</i> ⁵ D ₁ ^o ← <i>a</i> ⁵ D ₀)	392.1 (<i>z</i> ⁵ D ₁ ^o → <i>a</i> ⁵ D ₂)	1.9 ± 0.2
Cr(<i>z</i> ⁵ D ₄ ^o)	295.7 ^b	295.7 (<i>z</i> ⁵ D ₄ ^o ← <i>a</i> ⁷ S ₃)	391.9 (<i>z</i> ⁵ D ₄ ^o → <i>a</i> ⁵ D ₄)	2.9 ± 0.1
Cr(<i>y</i> ⁷ P ₃ ^o)	295.6 ^c	—	359.3 (<i>y</i> ⁷ P ₃ ^o → <i>a</i> ⁵ S ₃)	2.7 ± 0.2
Cr(<i>z</i> ⁷ P ₃ ^o)	295.6	—	427.5 (<i>z</i> ⁷ P ₃ ^o → <i>a</i> ⁵ S ₃)	2.8 ± 0.2

^aNon-resonant wavelengths for atomic transition. ^bResonant wavelength for the *z*⁵D₄^o ← *a*⁷S₃ atomic transition.

to be a polyatomic molecule.

B. Dependence of CL and LIF intensities on the photolysis laser power. To investigate precursors for the emitting species in the reaction cell, the CL intensities vs. photolysis laser power were monitored at three different wavelengths. The CL signal intensities monitored at 400, 500 and 640 nm, respectively, showed second-order dependence on the photolysis laser power as plotted in Figure 2(a). We have also investigated the photolysis laser power dependence of the LIF intensities for the low-lying energy states of Cr atoms produced in the reaction cell. The excitation and fluorescence wavelengths for the *a*⁷S₃, *a*⁵S₂ and *a*⁵D₁ states are shown in Table 1. As depicted in Figure 2(b), the LIF intensities from the *a*⁷S₃, *a*⁵S₂ and *a*⁵D₀ states also showed second-order dependence on the photolysis laser power. Thus, the dependence of the CL intensities as well as the LIF intensities from low-lying Cr atomic states on the photolysis laser power strongly supports that one of the reactants for the emitting species must be Cr atoms generated in the low-lying electronic states.

C. Dependence of CL intensities upon O₂ and Ar pressures. Premixed gases with 1, 2, 5, and 10% O₂ in Ar were prepared to investigate O₂ pressure dependence of the CL intensities. The premixed gases were used to entrap Cr(CO)₆ vapor maintaining the same flow rate and the total pressure of the cell was kept the same at 0.5 Torr. The pulse energy of photolysis laser was 0.5 mJ/pulse. The CL intensities monitored at 400 and 500 nm, respectively, showed first-order dependence on O₂ pressure when the O₂ partial pressure was in the 5–50 mTorr range as shown in Figure 3(a). Thus, the emitting species in this work must be formed by a direct reaction with O₂.

The dependence of the CL intensities upon Ar buffer gas pressure also was studied under static conditions. For this

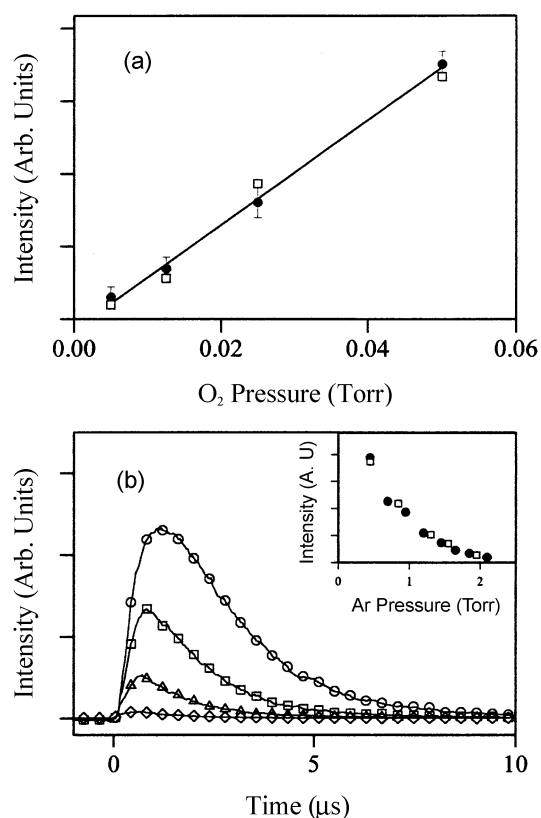


Figure 3. (a) Oxygen pressure dependence of CL intensities monitored at 400 (●) and 500 (□) nm, respectively. (b) Representative time profiles for the CL signal monitored at 400 nm vs. Ar buffer pressures: 0.45 (○), 0.95 (□), 1.45 (△), and 2.10 (◇) Torr of Ar. To avoid congestion, one data point from every 10 points is plotted. Time integrated CL intensities monitored at 400 (●) and 500 (□) nm vs. Ar pressure are shown in the insert of (b).

purpose, the premixed gas with 10% O₂ in Ar was used to entrap Cr(CO)₆ vapor, and the cell pressure was adjusted to 0.5 Torr before adding extra Ar to the cell. Typical time profiles monitored at 400 nm for different Ar pressures are plotted in Figure 3(b). As shown in the insert, the time integrated CL intensity decreased exponentially as the Ar pressure increased. When the decaying part of the time profiles were analyzed, we obtained relatively small apparent quenching rate constants for the CL signal by Ar as shown in Table 2. These results strongly imply that presence of excess

Table 2. Apparent radiative lifetime and quenching rate constant of the CrO₂* by O₂ and Ar^a

λ_{obs} (nm)	Pressure (Torr)			k_q (cm ³ molecule ⁻¹ s ⁻¹)	τ_{rad} (μs) ^b
	O ₂	Ar	Cr(CO) ₆		
400	0.05-0.65	0.45	0.0025	8.0 ± 0.5 × 10 ⁻¹¹	1.5 ± 0.2
	0.05	0.45-1.05	0.0025	6.2 ± 0.5 × 10 ⁻¹²	1.5 ± 0.2
500	0.05-0.65	0.45	0.0025	9.0 ± 0.5 × 10 ⁻¹¹	2.1 ± 0.2
	0.05	0.45-1.05	0.0025	6.3 ± 0.3 × 10 ⁻¹²	2.1 ± 0.2
320 ^c	> 0.0016				

^aThe composition of premixed gas was 10% O₂ in Ar. ^bCalculated from $1/\tau = 1/\tau_{\text{rad}} + k_q^{\text{Ar}}[\text{Ar}] + k_q^{\text{O}_2}[\text{O}_2]$. ^cThis band emission was reported in Ref. 29, but was not observed in this work.

Ar prevents the generation of the emitting species.

We also looked for the shapes of CL time profiles at higher O_2 pressures under static conditions. When O_2 pressure was increased while keeping $\text{Cr}(\text{CO})_6$ and Ar pressure constant, both the rise and decay time of the CL signal decreased. When the decay time vs. O_2 pressure was analyzed, the apparent quenching rate constants by O_2 were $8.0 \pm 0.5 \times 10^{-11}$ and $9.0 \pm 0.5 \times 10^{-11} \text{ cm}^3 \text{ molecule}^{-1} \text{ s}^{-1}$ for the 400 and 500 nm emissions, respectively. Although the apparent quenching rate constants by O_2 were much larger than those by Ar, the time integrated CL intensities in the presence of excess O_2 did not decrease as sharply as those for Ar. Based on the measured quenching rate constants by Ar and O_2 , the apparent radiative lifetimes of the emitting species calculated from Stern-Volmer plots were 1.5 ± 0.2 and $2.1 \pm 0.2 \mu\text{s}$ for the 400 and 500 nm emissions, respectively. The very long apparent radiative lifetimes suggest that the emission might be originated from such a spin forbidden transition.

D. Depletion rate constants of $\text{Cr}(a^7S_3)$, $\text{Cr}(a^5S_2)$, and $\text{Cr}(a^5D_0)$ atoms by O_2 . The variations of LIF intensities from the low-lying states of Cr atoms were monitored vs.

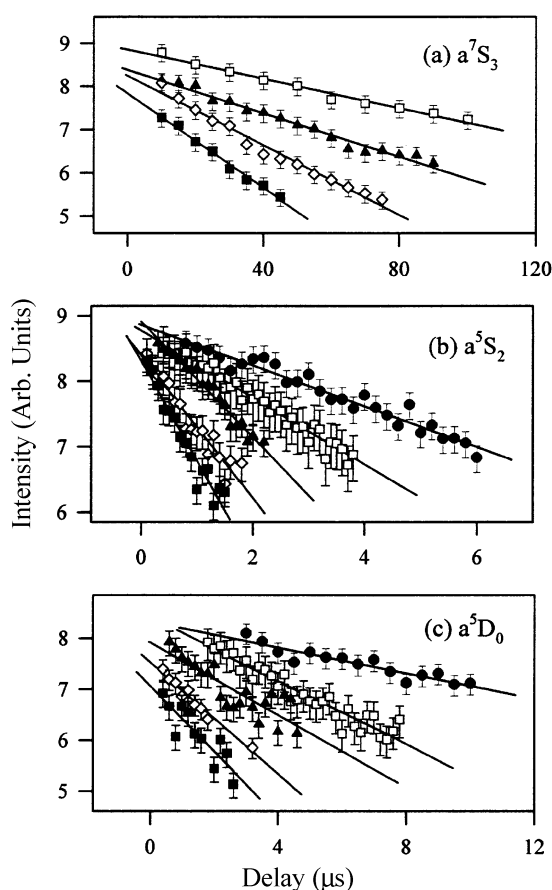


Figure 4. Dependence of LIF intensities of the low-lying atomic states of Cr atoms on the photolysis and probe delay time at different O_2 pressures. The partial pressures of $\text{Cr}(\text{CO})_6$ vapor and He were kept constant at 0.45 Torr. The partial O_2 pressures were (a) 0.25 (\square), 0.45 (\blacktriangle), 0.65 (\diamond), and 0.95 (\blacksquare) Torr, (b) 0.05 (\bullet), 0.25 (\square), 0.45 (\blacktriangle), 0.75 (\diamond), and 0.95 (\blacksquare) Torr, (c) 0.05 (\bullet), 0.25 (\square), 0.45 (\blacktriangle), 0.75 (\diamond) and 0.95 (\blacksquare) Torr, respectively.

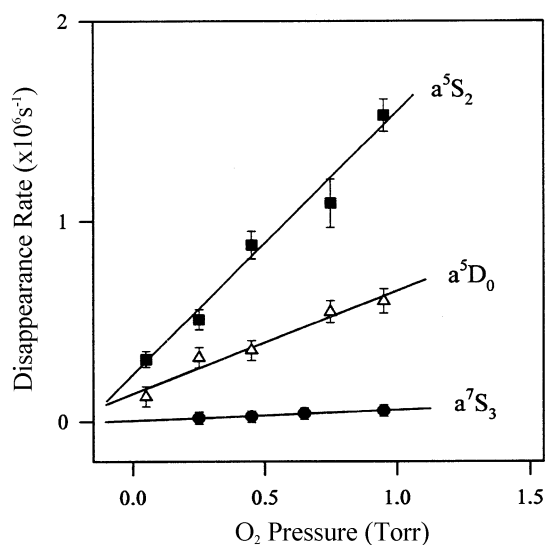


Figure 5. Oxygen pressure dependence of the disappearance rate for the low-lying atomic states of Cr atoms.

delay time between the photolysis and probe laser pulses at different oxygen pressures and plotted in Figure 4. The $\text{Cr}(\text{CO})_6$ vapor was entrapped using a 10% O_2 in He mixture. The pressure of the $\text{Cr}(\text{CO})_6/\text{O}_2/\text{He}$ mixture was kept constant at 0.5 Torr and additional O_2 was added to the photolysis/LIF cell. As shown in Figure 4, Cr atoms in the a^5S_2 and a^5D_0 states were depleted much faster than the ground state (a^7S_3). When the disappearance rates of the low-lying electronic states of Cr atoms vs. O_2 pressure were replotted as in Figure 5, the bimolecular removal rate constants were obtained. As shown in Table 3, the bimolecular removal rate constant for the $\text{Cr}(a^5S_2)$ state by O_2 is substantially larger than those for $\text{Cr}(a^7S_3)$ and $\text{Cr}(a^5D_0)$ even though the $\text{Cr}(a^5D_0)$ state locates at 158 cm^{-1} above the $\text{Cr}(a^5S_2)$ state.

E. Optical pumping of $\text{Cr}(a^5D_4)$ and CL intensities. The population of Cr atoms in the a^5D_4 state was increased intentionally by optical pumping to look for any change in the intensities of the CL signal. Since the Einstein A coefficient for $z^5D_4^o \rightarrow a^5D_4$ transition is fairly large,²¹ and since the $z^5D_4^o$ state can be generated directly by the photolysis laser pulse, the population in the a^5D_4 state can be increased by photolyzing the gas mixture using $z^5D_4^o \leftarrow a^7S_3$ atomic transition frequency. Figure 6(a) shows the variation

Table 3. Removal rate constants for the low-lying electronic states of Cr by O_2

State	λ_{exc} (nm) (Transition)	λ_{obs} (nm) (Transition)	Rate constants ^a ($\text{cm}^3 \text{ molecule}^{-1} \text{ s}^{-1}$)
a^7S_3	373.2 ($z^5P_3^o \leftarrow a^7S_3$)	520.8 ($z^5P_3^o \rightarrow a^5S_2$)	$1.7 \pm 0.3 \times 10^{-12}$
a^5S_2	387.0 ($z^5D_1^o \leftarrow a^5S_2$)	392.1 ($z^5D_1^o \rightarrow a^5D_2$)	$4.0 \pm 0.6 \times 10^{-11}$
a^5D_0	389.4 ($z^5D_1^o \leftarrow a^5D_0$)	392.1 ($z^5D_1^o \rightarrow a^5D_2$)	$1.6 \pm 0.3 \times 10^{-11}$

^aMeasured in the presence of 0.45 Torr He.

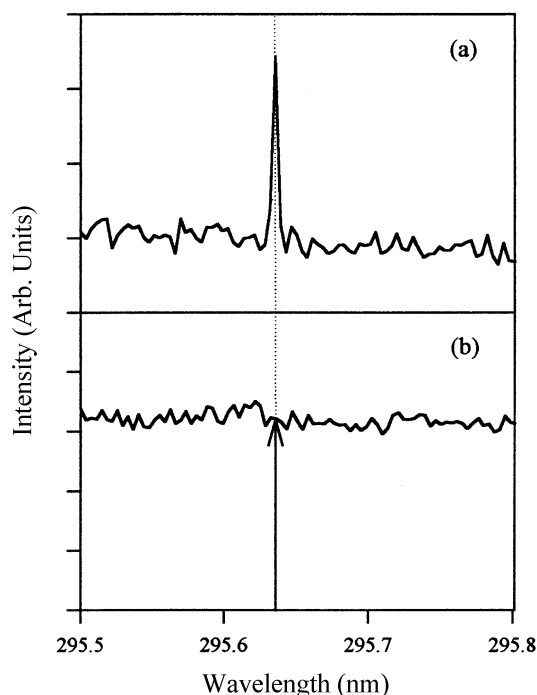


Figure 6. (a) Population change of $\text{Cr}(a^5D_4)$ atoms by changing the photolysis laser wavelength. The probe laser frequency was set at $z^5D_4^o \leftarrow a^5D_4$ transition (391.9 nm) and the fluorescence from $z^5D_4^o \rightarrow a^5D_3$ transition was monitored at 388.8 nm. The delay time between photolysis and probe pulses was 2 μs . (b) Intensities of the CL signal monitored at 500 nm vs. photolysis laser wavelength. A 10% O_2 in He mixture was slowly flowed over $\text{Cr}(\text{CO})_6$ powder at 273 K and the total pressure in the cell was 0.5 Torr.

of the a^5D_4 state population vs. photolysis laser wavelength, which was probed at 2 ms after the photolysis laser pulse. The probe laser wavelength was 391.9 nm ($z^5D_4^o \leftarrow a^5D_4$) and the fluorescence from the $z^5D_4^o \rightarrow a^5D_3$ transition was monitored at 388.8 nm. It is seen that the population of the a^5D_4 state can be increased by 3.5 times at 295.64 nm. The CL intensities shown in Figure 6(b), however, remain effectively the same. Thus, the a^5D_1 state seems not responsible for the CL signal based on this optical pumping experiment.

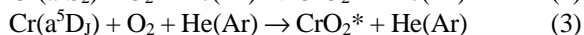
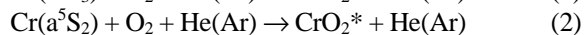
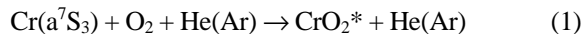
Discussion

The first-order dependence of CL intensities upon O_2 pressure and absence of CL signal from $\text{Cr}(\text{CO})_6/\text{N}_2\text{O}/\text{He}$ mixtures support that O_2 is one of the primary reactants. Also, the second-order dependence of both CL and LIF intensities for those a^7S_3 , a^5S_2 , and a^5D_1 states of Cr atoms on the photolysis laser power supports that the CL intensities derive from the low-lying states of Cr atoms. Thus, the chemical species that gives CL signal must be a product from direct reactions of O_2 and low-lying states of Cr atoms. Since photodissociation of gas-phase $\text{Cr}(\text{CO})_6$ by UV laser is very fast,^{23,24} we ruled out the $\text{Cr}(\text{CO})_x^*$ ($x=1-6$) intermediate species generated by two-photon absorption as a plausible reactant for the emitting species in this work.

The CL spectra in Figure 1 is completely different from

that of CrO^* produced from the reaction of Cr atoms with O_3 reported by Devore and Gole.²⁵ The reaction of $\text{Cr}(a^7S_3)$ with O_3 is highly exothermic to generate electronically excited states of CrO, while the reaction of $\text{Cr}(a^7S_3)$ with O_2 is 0.38 ± 0.09 eV endothermic to generate ground state CrO.¹⁰ Since the three low-lying atomic states are generated dominantly by two-photon absorption, the maximum available kinetic energies are about 1.7 eV for the $\text{Cr}(a^7S_3)$ atoms and about 0.8 eV for the $\text{Cr}(a^5S_2)$ and $\text{Cr}(a^5D_0)$ atoms, considering the energy required for complete dissociation of six carbonyl groups is 6.68 eV.^{26,27} The actual kinetic energies of the Cr atoms should be much smaller than the maximum available kinetic energies since the CO fragments take away substantial amount (< 0.5 eV) of the absorbed energies.^{27,28} Thus, the CL species in this work cannot be CrO^* , because the available energy is not sufficient to generate CrO^* . The absence of CL signal from $\text{Cr}(\text{CO})_6/\text{N}_2\text{O}/\text{He}$ mixtures also supports this argument because the reaction of $\text{Cr}(a^7S_3)$ with N_2O to generate CrO is highly exothermic.

If the emitting species are direct products from reactions of Cr atoms with O_2 , only plausible candidate is CrO_2^* generated by the following reactions.



However, as shown in Figure 6, 3.5 times increased population of $\text{Cr}(a^5D_4)$ atoms by optical pumping did not affect the CL intensities. We also attempted to increase the population of $\text{Cr}(a^5S_2)$ atoms by optical pumping, but the CL intensities were not affected. Thus, the optical pumping results suggest that Eqs. (2) and (3) are not the major channel for the formation of CrO_2^* in this work, although we cannot rule out Eqs. (2) and (3) completely.

Martinez has studied the reaction of a $\text{Cr}(a^7S_3)$ atom with H_2 , N_2 , and O_2 using a density functional theory.³ He has reported that the reaction of a $\text{Cr}(a^7S_3)$ atom with ground state O_2 is highly exothermic and the ground state $\text{CrO}_2(X^3B_2)$ is located at 525.5 kJ/mol below the dissociation limit. He has also found that there exist thermodynamically stable CrO_2 molecular states locating at 124.3, 134.7, 219.7, 337.2, 340.2, and 466.5 kJ/mol, respectively, below the dissociation limit. Thus, the CL emissions observed in this work are energetically in the plausible range among the various CrO_2 molecular states generated from the reaction of the ground state Cr atom with O_2 .

Parnis and co-workers have studied the reaction (1) in the presence of large amount of Ar buffer gas, but they did not observe chemiluminescence or LIF from ground state CrO molecules.¹⁷ They have monitored the disappearance rate of $\text{Cr}(a^7S_3)$ atoms at various Ar pressures, and shown that the pseudo-second-order rate constant for removal of the ground state $\text{Cr}(a^7S_3)$ atoms by O_2 depends on the Ar buffer gas pressure. They concluded that the $\text{Cr}(a^7S_3)$ atoms react readily with O_2 to form CrO_2 association complex based on their large termolecular rate constant. Although we did not measure the removal rate constants for $\text{Cr}(a^7S_3)$ atoms by O_2

at different buffer gas pressures in this work, the rate constant measured in the presence of 0.45 Torr of He is in accord with the results of Parnis and co-workers, when their data are extrapolated to lower buffer gas pressures. Nevertheless, Parnis and co-workers did not detect CL signal. As shown in Figure 3(b), the CL intensities were very sensitive to Ar pressure. This sensitive dependence of CL intensities on Ar pressure manifest itself why Parnis and co-workers did not succeed to observe any CL signal under their experimental conditions.

The shapes of CL time profiles shown in Figure 3(b), the results of optical pumping, and no detection of CL signal by Parnis and co-workers can be qualitatively explained if we assume that hot ground state Cr atoms generated by two-photon dissociation of Cr(CO)₆ at relatively low pressures react with O₂ to form CrO₂* which gives CL signal in this work. Then, at higher Ar buffer gas pressures, fast collisional cooling of hot Cr atoms may prevent the formation of CrO₂*. At higher partial pressures of O₂, increased collision probabilities between the hot ground state Cr atoms and O₂ would decrease the rise time of the CL signal, however, O₂ might also quench CrO₂* quite effectively. Also, the optical pumping of a⁵D₄ atoms may not affect the CL intensities if hot ground state Cr atoms are responsible for the CL, because only a minor portion of the ground state population can be optically pumped using a UV laser with ~10 ns pulse width.

To confirm these arguments, we have looked for the variation of Doppler line width of the z⁵D₄ ← a⁷S₃ absorption spectrum vs. delay time. As plotted in Figure 7, the z⁵D₄

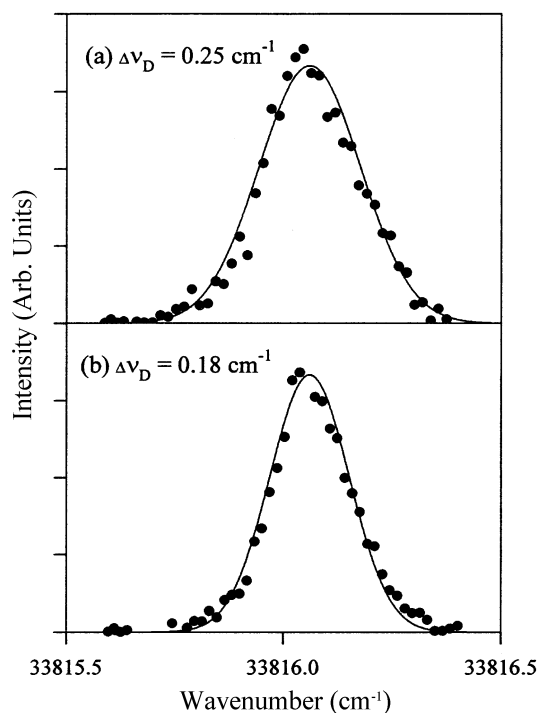
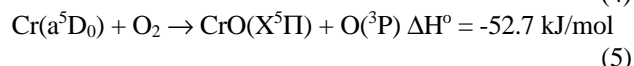
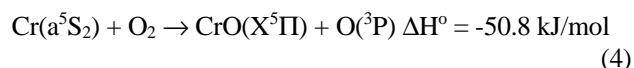


Figure 7. The z⁵D₄ ← a⁷S₃ absorption line profile at different delay time. The delay time between the photolysis and probe pulses was (a) 0 μs and (b) 5 μs. The Ar gas was slowly flowed over Cr(CO)₆ powder at 273 K and the cell pressure was 2.0 Torr.

← a⁷S₃ absorption line width at 2.0 Torr was much broader than the excitation laser line width of ~0.1 cm⁻¹ (FWHM), and decreased substantially at 5 μs delay time. When the observed Doppler line profiles were deconvoluted for the excitation laser line width (0.1 cm⁻¹), the Gaussian Doppler width (FWHM) with 0.25 and 0.18 cm⁻¹, respectively, were fitted fairly well for the experimental profiles at zero and 5 μs delay times, respectively. The Doppler width at zero delay time corresponded to a translational temperature of 6200 ± 500 K, which is in accord with Tyndall and Jackson.²² On the other hand, the Doppler width at 5 μs delay time corresponded to a translational temperature of 2900 ± 700 K indicating fast collisional cooling subsequent to the formation of hot Cr(a⁷S₃) atoms. Although we did not investigate the Doppler width of the Cr(a⁵S₂) and Cr(a⁵D₀) atoms generated by two-photon absorption of Cr(CO)₆, they should possess much smaller kinetic energies than the Cr(a⁷S₃) atoms and formation of CrO₂* might be unfavorable. However, considering the relatively fast disappearance rate constant which corresponds to the sum of physical and chemical quenching of the Cr(a⁵S₂) and Cr(a⁵D₀) atoms, following exothermic reactions seem to be one of the exit channel.²⁹



The larger disappearance rate constant for the a⁵S₂ state (4s¹3d⁵) which locates 158-715 cm⁻¹ lower in energy than the a⁵D_J state (4s²3d⁴) may reflect that TM atoms having s¹dⁿ⁻¹ electron configuration are more reactive than those having s²dⁿ⁻² electron configuration.⁵

Parson has reported a CL spectrum peaked at ~320 nm from his beam-gas experiment with Cr + O₂, and concluded that the chemical species responsible for the observed CL spectrum is CrO₂* generated by a two-body radiative recombination (2BRR) mechanism.³⁰ We have also attempted to look for the CL band peaked at ~320 nm, but the CL intensities in the 300-350 nm region are very weak under our experimental conditions. Although the spectral range and overall shape of the CL spectrum in Figure 1 are much different from the Parson's spectrum, the first-order dependence of CL intensities on O₂ pressure and the suppression of CL intensities by the presence of excess Ar suggest that the CL signal in this work might be another example of 2BRR. It is difficult to explain the nature of different CL spectra reported by Parson and in this work, since the excited state potential surfaces of CrO₂ molecules are not available yet.

Acknowledgement. This work was supported by Korea Research Foundation Grant (KRF-2000-015-DP0214) and BK 21.

References

1. Campbell, M. L.; Kölsch, E. J.; Hooper, K. L. *J. Phys. Chem. A* 2000, 104, 11147.

2. Chertihin, G. V.; Bare, W. D.; Andrews, L. *J. Chem. Phys.* **1997**, *107*, 2798.
 3. Martínez, A. *J. Phys. Chem. A* **1998**, *102*, 1381.
 4. Ritter, D.; Weisshaar, J. C. *J. Phys. Chem.* **1989**, *93*, 1576.
 5. Brown, C. E.; Mitchell, S. A.; Hackett, P. A. *J. Phys. Chem.* **1991**, *95*, 1062.
 6. Futerko, P. M.; Fontijn, A. *J. Chem. Phys.* **1991**, *95*, 8065.
 7. Campbell, M. L.; McClean, R. E.; Harter, J. S. *Chem. Phys. Lett.* **1995**, *235*, 497.
 8. Matsui, R.; Senba, K.; Honma, K. *Chem. Phys. Lett.* **1996**, *250*, 560.
 9. Parson, J. M.; Geiger, L. C.; Conway, T. J. *J. Chem. Phys.* **1981**, *74*, 5595.
 10. Hedgecock, I. M.; Naulin, C.; Coates, M. *Chem. Phys. Lett.* **1996**, *207*, 379.
 11. Akhmadov, U. S.; Zaslono, I. S.; Smirnov, V. N. *Kinet. Catal.* **1988**, *29*, 251.
 12. Helmer, M.; Plane, J. M. C. *J. Chem. Soc. Faraday Trans.* **1994**, *90*, 31.
 13. Chalek, C. L.; Gole, J. L. *Chem. Phys.* **1977**, *19*, 59.
 14. Dubois, L. H.; Gole, J. L. *J. Chem. Phys.* **1977**, *66*, 779.
 15. Jones, R. W.; Gole, J. L. *J. Chem. Phys.* **1976**, *65*, 3800.
 16. Ritter, D.; Weisshaar, J. C. *J. Phys. Chem.* **1990**, *94*, 4907.
 17. Parnis, J. M.; Mitchell, S. A.; Hackett, P. A. *J. Phys. Chem.* **1990**, *94*, 8152.
 18. (a) Son, H. S.; Lee, K.; Shin, S. K.; Ku, J. K. *Chem. Phys. Lett.* **2000**, *320*, 658. (b) Son, H. S.; Lee, K.; Kim, S. B.; Ku, J. K. *Bull. Korean Chem. Soc.* **2000**, *21*, 583.
 19. Son, H. S.; Ku, J. K. *Bull. Korean Chem. Soc.* **2002**, *23*, 184.
 20. Moore, C. E. Atomic Energy levels as Derived from the Analysis of Optical Spectra. Vol. II; *Natl. Stand. Ref. Data Ser. (U.S., Natl. Bur. Stand.)* **1971**, NSRDS-NBS 35.
 21. Martin, G. A.; Fuhr, J. R.; Wiese, W. L. *J. Phys. Chem. Ref. Data* **1988**, *17*, Suppl. 3.
 22. Tyndall, G. W.; Jackson, R. L. *J. Chem. Phys.* **1988**, *89*, 1364.
 23. (a) Trushin, S. A.; Fuss, W.; Schmid, W. E.; Kompa, K. L. *J. Phys. Chem. A* **1998**, *102*, 4129. (b) Gutmann, M.; Janello, J. M.; Dickebohm, M. S.; Grossekathefer, M.; Lindener-Roenneke, J. *J. Phys. Chem. A* **1998**, *102*, 4138.
 24. Jackson, R. L. *Acc. Chem. Res.* **1992**, *25*, 581.
 25. Devore, T. C.; Gole, J. L. *Chem. Phys.* **1989**, *133*, 95.
 26. Pilcher, G.; Ware, M. J.; Pittam, D. A. *J. Less-Common Met.* **1975**, *42*, 223.
 27. Peifer, W. R.; Garvey, J. F. *J. Chem. Phys.* **1991**, *94*, 4821.
 28. (a) Waller, I. M.; Hepburn, J. W. *J. Chem. Phys.* **1988**, *88*, 6658. (b) Waller, I. M.; Davis, H. F.; Hepburn, J. W. *J. Phys. Chem.* **1987**, *91*, 506.
 29. Chase, M. W., Jr.; Davies, C. A.; Downey, J. R., Jr.; Frurip, D. J.; McDonald, R. A.; Syverud, A. N. *J. Phys. Chem. Ref. Data* **1985**, *14*, Suppl. 1. (JANAF Thermochemical Table)
 30. Parson, J. M. *J. Phys. Chem.* **1986**, *90*, 1811.
-